exchange of carbonyl groups. As shown in Scheme III there are several plausible intermediates which would allow for carbonyl group migration between Fe and Rh. We favor the doubly bridged structure F since it is easily achieved from both isomeric C and D and it maintains the favored μ-η^4,η^3-C_7H_7 bonding functionality. Furthermore, the process is related to the well-established merry-go-round mechanism for carbonyl group migration in di- and polynuclear metal carbonyl compounds.[32] An often observed feature in these systems is increased facility for carbonyl group migration upon phosphine substitution.[32,36] This is well illustrated in the present context as well. The parent pentacarbonyl **1a** shows no line broadening in the ^{13}C NMR spectrum up to 70 °C whereas in **1b** this temperature represents the coalescence point with an associated $\Delta G^{\ddagger}_{343}$ of 15.4 kcal/mol.

Conclusion

It is apparent from this first reactivity study on **1a** that the bridging cycloheptatrienyl moiety is capable of exhibiting a variety of bonding capabilities. This flexible nature can be manifested in two distinct manners. The ability to create coordinative unsaturation is responsible for the facile carbonyl substitution reaction and may promote other reactions as well. The capacity for bonding mode changes between the Fe–Rh framework and the μ-C_7H_7 ligand is the reason for the movement of terminal CO group to bridging position and the associated CO scrambling processes.

Further studies are underway to delineate the scope of the reactivity of **1a**. The synthesis of related (μ-C_7H_7)-$MM'(CO)_5$ (M = Fe, Ru, Os and M′ = Co, Rh, Ir) compounds are also being explored in order to probe the effect of the metal on the structure, fluxionality, and reactivity in this class of molecules.

Acknowledgment. We thank the Natural Sciences and Engineering Research Council of Canada and the University of Alberta for financial support of this work and Johnson Matthey for generous loan of rhodium trichloride. F.E. acknowledges a Feodor Lynen research fellowship from the Alexander von Humboldt Foundation, Bonn, West Germany.

Registry No. **1a**, 51608-48-1; **1b**, 100190-09-8; **2a**, 91868-00-7; **2b**, 91855-30-0; **3a**, 91855-31-1; **3b**, 91855-32-2; **3c**, 91855-33-3; **3d**, 91855-34-4; **3e**, 100190-10-1; **3f**, 100190-11-2; $Na(C_7H_7)Fe(CO)_3$, 62313-81-9; $[RhCl(COD)]_2$, 12092-47-6; Rh, 7440-16-6; Fe, 7439-89-6.

Supplementary Material Available: A table of thermal parameters for **1b** (Table VIII) and listings of observed and calculated structure amplitudes for **1b** and **3b** (31 pages). Ordering information is given on any current masthead page.

(36) Mersalla, J. A.; Caulton, K. G. *Organometallics* 1982, *1*, 274.

Synthesis, Molecular Structure, Solution Dynamics, and Reactivity of (η-C_5H_5)$_2$M(μ-PR_2)$_2$Rh(η-indenyl) (M = Zr, Hf; R = Et, Ph)[†]

R. T. Baker* and T. H. Tulip

Central Research & Development Department, E. I. du Pont de Nemours & Company, Experimental Station, Wilmington, Delaware 19898

Received June 13, 1985

The "metal-containing diphosphines", $Cp_2M(PR_2)_2$ (Cp = η-C_5H_5; M = Zr, Hf; R = Et, Ph), displace both coordinated ethylenes from (η-C_2H_4)$_2$Rh(η-indenyl), yielding the early–late heterobimetallic complexes Cp_2M(μ-PR_2)$_2$Rh(η-indenyl). The molecular structure of Cp_2Zr(μ-PPh_2)$_2$Rh(η-indenyl) (**1c**), determined by X-ray diffraction, consists of edge-shared, pseudotetrahedral 16e Zr(IV) and distorted, square-planar Rh(I) centers with a planar ZrP_2Rh bridging unit and a Zr···Rh separation of 3.088 (1) Å. The indenyl ligand exhibits a pronounced "slip-fold" distortion toward η^3-coordination and high barriers (14–15 kcal/mol) to indenyl rotation are observed by ^1H DNMR. Addition of CH_3I to Cp_2M(μ-PEt_2)$_2$Rh(η-indenyl) affords the cationic d^0–d^6 heterobimetallics [Cp_2M(μ-PEt_2)$_2$Rh (CH_3)(η-indenyl)]I. Red crystals of **1c** are monoclinic, $P2_1/m$ (no. 11), with two molecules per unit cell of dimensions a = 9.700 (1) Å, b = 18.855 (3) Å, c = 10.185 (1) Å, and β = 112.95 (1)°. The structure was refined to R = 0.029 and R_w = 0.031 for 2928 observed reflections.

Transition-metal complexes containing the η-indenyl ligand undergo ligand substitution much more readily than their η-cyclopentadienyl analogs due to the stability of the η^3 bonding mode in the former, suggested to result from the aromatization of the indenyl benzene ring.[1] The recently reported[2,3] "metal-containing diphosphines", $Cp_2M(PR_2)_2$ (Cp = η-C_5H_5; M = Zr, Hf; R = Et, Ph, cyclohexyl (Cy)), contain both 1e and 3e donor PR_2 ligands. Donation of both phosphorus lone pairs to a second metal center thus creates an electronically unsaturated early metal center in the resulting PR_2-bridged heterobimetallic complex. We have previously described the binding of various metal carbonyl[4] and ML_n[5] fragments, where M = Ni, Pd,

† Contribution no. 3775.

(1) (a) Hart-Davis, A. J.; Mawby, R. J. *J. Chem. Soc. A* **1969**, 2403. (b) White, C.; Mawby, R. J.; Hart-Davis, A. J. *Inorg. Chim. Acta* **1970**, *4*, 441. (c) Jones, D. J.; Mawby, R. J. *Ibid.* **1972**, *6*, 157. (d) Eshtiagh-Hosseini, H.; Nixon, J. F. *J. Less Common Met.* **1978**, *61*, 107. (e) Caddy, P.; Green, M.; O'Brien, E.; Smart, L. E.; Woodward, P. *Angew. Chem., Int. Ed. Engl.* **1977**, *16*, 648; *J. Chem. Soc., Dalton Trans.* **1980**, 962. (f) Caddy, P.; Green, M.; Howard, J. A. K.; Squire, J. M.; White, N. J. *Ibid.* **1981**, 400. (g) Bottrill, M.; Green, M. *Ibid.* **1977**, 2365. (h) Gal, A. W.; van der Heijden, H. *Angew. Chem., Int. Ed. Engl.* **1981**, *20*, 978. (i) Diversi, P.; Giusti, A.; Ingrosso, G.; Lucherini, A. *J. Organomet. Chem.* **1981**, *205*, 239. (j) Rerek, M. E.; Ji, L.-N.; Basolo, F. *J. Chem. Soc., Chem. Commun.* **1983**, 1208. (k) Rerek, M. E.; Basolo, F. *J. Am. Chem. Soc.* **1984**, *106*, 5908. (l) Casey, C. P.; O'Connor, J. M. *Organometallics* **1985**, *4*, 384.

0276-7333/86/2305-0839$01.50/0

Table I. Elemental Analyses and Melting Point Data

	no.	mp, °C	elemental analyses[a,b] C	H	P	Rh	M	I
			$Cp_2M(\mu\text{-}PR_2)_2Rh(\eta\text{-indenyl})$					
M = Zr, R = Et	**1a**	295–297	51.97, 52.17 (52.50)	6.08, 6.11 (6.04)	9.91, 10.10 (10.03)	16.6, 16.8 (16.66)	14.8, 14.9 (14.77)	
M = Hf, R = Et	**1b**	295–297	45.77, 45.70 (46.00)	5.21, 5.23 (5.29)	8.68, 8.73 (8.79)	14.5, 14.5 (14.60)	24.6, 24.7 (25.32)	
M = Zr, R = Ph	**1c**	270–272	63.17, 62.88 (63.77)	4.66, 4.60 (4.61)	7.40, 7.51 (7.65)	12.7, 12.6 (12.71)	11.8, 11.7 (11.26)	
M = Hf, R = Ph	**1d**	280–285	57.79, 57.82 (57.57)	4.48, 4.53 (4.16)	6.53, 6.71 (6.91)	11.0, 11.0 (11.47)	18.4, 18.6 (19.90)	
			$[Cp_2M(\mu\text{-}PEt_2)_2Rh(CH_3)(\eta\text{-indenyl})]I$					
M = Zr	**2a**	162–165	44.12, 43.99 (44.27)	5.28, 5.29 (5.31)	7.94, 7.95 (8.16)	13.5, 13.5 (13.55)	12.0, 12.0 (12.01)	16.6, 16.7 (16.71)
M = Hf	**2b**	165–168	39.10, 39.13 (39.71)	4.75, 4.75 (4.76)	7.32, 7.17 (7.31)	12.2, 11.9 (12.15)	20.9, 20.2 (21.08)	14.3, 14.3 (14.99)

[a] Found; calculated in parentheses. [b] Hf analyses are low due to significant quantities of Cp_2ZrCl_2 in commercial Cp_2HfCl_2.

and Pt, L = diene, alkyne, phosphine, diphosphine, and phosphite, and n = 1 and 2. We now report (i) the binding of the Rh(η-indenyl) fragment, (ii) the X-ray structural determination of $Cp_2Zr(\mu\text{-}PPh_2)_2Rh(\eta\text{-indenyl})$, (iii) the observation of hindered indenyl ligand rotation in solution by ^1H DNMR, and (iv) the oxidative addition of CH_3I to the Rh(I) center without disruption of the MP_2Rh bridge system.

Experimental Section

All operations were conducted in a Vacuum Atmospheres glovebox with continuous nitrogen flush. Solvents were purified by standard techniques[6] and distilled from sodium– or potassium–benzophenone ketyl. (η-Indenyl)Rh(η-C_2H_4)$_2$[1d,e] and $Cp_2M(PR_2)_2$[2,4] were prepared by literature methods. CH_3I, $CH_3C(O)Cl$, NH_4PF_6 (Aldrich), and research purity H_2 and CO (Matheson) were used as received. NMR spectra were recorded on a Nicolet NMC-300-WB (121-MHz ^{31}P and 76-MHz ^{13}C) spectrometer. ^{13}C and ^{31}P NMR chemical shifts are positive downfield from external $SiMe_4$ and 85% H_3PO_4, respectively. IR spectra were recorded as Nujol mulls between CsI plates on a Perkin-Elmer 983 spectrometer. Elemental analyses were performed by Pascher Mikroanalytisches Labor, Bonn, West Germany. Melting points were determined in sealed, nitrogen-filled capillaries using a Thomas-Hoover apparatus and are uncorrected. Elemental analyses and melting points are listed in Table I, and IR and NMR data are compiled in Tables II–V.

$Cp_2Zr(\mu\text{-}PEt_2)_2Rh(\eta\text{-indenyl})$ (1a). To a solution of 1.199 g (3.0 mmol) of $Cp_2Zr(PEt_2)_2$ in 60 mL of hexane was added dropwise a solution of 823 mg (3.0 mmol) (η-indenyl)Rh(η-C_2H_4)$_2$ in 20 mL of hexane, over 10 min. The solution turned red-brown and slowly precipitated an orange solid. After the solution was stirred for 12 h, the product was filtered off, washed with 2 × 10 mL of cold (−30 °C) pentane, and dried in vacuo, yielding 1.333 g. Concentration of the filtrate to 5 mL yielded a second crop of 270 mg, for a combined yield of 1.603 g (87%). The Hf analogue **1b** was prepared similarly by using 1.461 g (3.0 mmol) of $Cp_2Hf(PEt_2)_2$, affording 1.814 g of product (86%). Red crystals of both complexes were obtained in good yield from toluene–heptane.

$Cp_2Zr(\eta\text{-}PPh_2)_2Rh(\eta\text{-indenyl})$ (1c). To a solution of 1.775 g (3.0 mmol) of $Cp_2Zr(PPh_2)_2$ in 40 mL of THF was added dropwise a solution of 823 mg (3.0 mmol) of (η-indenyl)Rh(η-C_2H_4)$_2$ in 40 mL of THF, over 10 min. The resulting dark red solution was stirred for 3 days and evaporated to dryness. The residue was stirred with 25 mL of hexane, filtered off, and dried in vacuo, yielding 2.191 g of the title product (90%). The Hf analogue **1d** was prepared similarly by using 2.037 g (3.0 mmol) of $Cp_2Hf(PPh_2)_2$, affording 2.415 g of product (90%). Red crystals of both complexes were obtained in good yield from THF–heptane.

$[Cp_2Zr(\mu\text{-}PEt_2)_2Rh(CH_3)(\eta\text{-indenyl})]I$ (2a). To a solution of 93 mg (0.15 mmol) of **1a** in 10 mL of hexane was added 21 mg (0.15 mmol) of CH_3I. The solution lightened and precipitated a yellow powder. After the solution was stirred for 12 h, the

Table II. Infrared Spectral Data[a]

$Cp_2Zr(\mu\text{-}PEt_2)_2Rh(\eta\text{-indenyl})$ (**1a**): 1316 (m), 1228 (m), 1208 (w), 1168 (w), 1146 (w), 1120 (w), 1066 (w), 1030 (s), 1022 (s), 1010 (s, sh), 975 (m), 924 (m), 885 (m), 877 (m), 851 (w), 843 (w), 823 (m, sh), 800 (s, sh), 791 (vs), 780 (vs), 765 (s), 736 (s), 721 (s), 673 (m), 633 (m), 438 (s), 398 (w), 386 (w, sh), <u>338</u> (m), 280 (w), 248 (w) cm^{-1}

$Cp_2Hf(\mu\text{-}PEt_2)_2Rh(\eta\text{-indenyl})$ (**1b**): 1315 (m), 1227 (m), 1208 (w), 1167 (w), 1158 (w), 1145 (w), 1120 (w), 1067 (w), 1029 (s), 1021 (s), 1010 (s), 976 (m), 924 (m), 884 (m), 875 (m), 851 (w), 844 (w), 828 (m), 805 (s, sh), 796 (vs), 780 (vs), 763 (vs), 735 (vs), 721 (s), 672 (m), 633 (m), 610 (w), 437 (s), 400 (w), 340 (w), 302 (w, sh), <u>286</u> (m), 246 (w) cm^{-1}

$Cp_2Zr(\mu\text{-}PPh_2)_2Rh(\eta\text{-indenyl})$ (**1c**): 1579 (m), 1564 (w), 1322 (w), 1310 (m), 1223 (m), 1213 (w), 1185 (w), 1174 (w), 1154 (w), 1120 (w), 1087 (w), 1070 (m, sh), 1062 (m), 1017 (s), 975 (m), 928 (m), 920 (m, sh), 892 (w), 854 (w), 843 (w), 831 (m), 811 (s), 790 (s), 781 (s), 736 (vs), 705 (s), 696 (s), 618 (w), 515 (s), 484 (s), 459 (m), 442 (w), 432 (w), 400 (m), 375 (w), 341 (w), <u>325</u> (w), 273 (w), 241 (w) cm^{-1}

$Cp_2Hf(\mu\text{-}PPh_2)_2Rh(\eta\text{-indenyl})$ (**1d**): 1577 (m), 1562 (w), 1321 (w), 1309 (m), 1222 (w), 1231 (w), 1184 (w), 1173 (w), 1153 (w), 1119 (w), 1087 (w), 1068 (w, sh), 1061 (m), 1015 (s), 978 (m), 926 (m), 890 (w), 845 (w, sh), 836 (m), 814 (s), 787 (s, sh), 782 (vs), 731 (vs), 703 (s, sh), 694 (s), 619 (w), 515 (s), 483 (s), 459 (m), 443 (m), 433 (m), 399 (m), 375 (w), 337 (w), <u>302</u> (w), 275 (w), 239 (w) cm^{-1}

$[Cp_2Zr(\mu\text{-}PEt_2)_2Rh(CH_3)(\eta\text{-indenyl})]I$ (**2a**): 3049 (m), 1541 (w), 1323 (w), 1237 (m), 1192 (w), 1183 (w), 1149 (m), 1121 (w), 1037 (s), 1020 (s), 975 (m), 946 (w), 926 (w), 892 (w), 861 (m), 850 (m), 838 (m), 828 (s), 809 (vs), 778 (m), 758 (s), 733 (s), 684 (s), 639 (m), 546 (w), 512 (w), 459 (m), 423 (w), 404 (w), 387 (w), <u>364</u> (w), 339 (w), 283 (w), 250 (w) cm^{-1}

$[Cp_2Hf(\mu\text{-}PEt_2)_2Rh(CH_3)(\eta\text{-indenyl})]I$ (**2b**): 3050 (m), 1540 (w), 1324 (w), 1237 (m), 1213 (w), 1192 (w, sh), 1184 (m), 1170 (w), 1151 (m), 1123 (w), 1036 (s), 1020 (s), 975 (m), 945 (w), 931 (w), 920 (w), 890 (w), 863 (m, sh), 854 (m), 841 (s, sh), 833 (s), 812 (vs), 777 (m), 758 (s), 731 (s), 684 (m), 640 (m), 545 (w), 512 (s), 456 (m), 421 (m), 404 (m), 386 (w), 336 (w), <u>315</u> (w), 281 (w), 247 (w) cm^{-1}

[a] Recorded as mineral oil mulls between CsI plates. Underlined absorptions are assigned to M–P vibrations.

(2) Baker, R. T.; Whitney, J. F.; Wreford, S. S. *Organometallics* **1983**, *2*, 1049; *Inorg. Chem.*, submitted for publication.
(3) Wade, S. R.; Wallbridge, M. G. H.; Willey, G. R. *J. Chem. Soc., Dalton Trans.* **1983**, 2555.
(4) Baker, R. T.; Tulip, T. H.; Wreford, S. S. *Inorg. Chem.* **1985**, *24*, 1379.
(5) Baker, R. T.; Fultz, W. C. *Organometallics*, to be submitted for publication.
(6) Gordon, A. J.; Ford, R. A. "The Chemist's Companion"; Wiley-Interscience: New York, 1972.

Table III. 301-MHz ^{1}H NMR Data[a]

1. $Cp_2M(\mu\text{-}PEt_2)_2Rh(\eta\text{-indenyl})$

			Et		indenyl			
M	no.	T, °C	CH_2	CH_3[b]	$H_{4\text{-}7}$[c]	$H_{1,3}$[d]	H_2[e]	Cp
Zr	**1a**	95[f]	1.9 (br, ov), 1.80 (mult)	1.26 (d tr, 14.5, 7.0)	6.77, 6.54	5.82 (2.5)	6.36 (2.5)	4.99
		−60[g]	2.82 (mult), 2.30 (mult), 1.23 (ov mult), 0.76 (mult)	1.37 (mult) 1.19 (ov mult)	6.75, 6.50	5.86 (2.0)	6.43 (2.0)	5.26, 4.65
Hf	**1b**	95[f]	1.9 (br, ov), 1.76 (mult)	1.26 (d tr, 14.0, 7.0)	6.77, 6.53	5.80 (2.5)	6.35 (2.5)	4.96
		−60[g]	2.92 (mult), 2.27 (mult), 1.2 (ov mult), 0.75 (mult)	1.38 (mult) 1.21 (ov mult)	6.76, 6.51	5.84	6.43	5.25, 4.65

2. $Cp_2M(\mu\text{-}PPh_2)_2Rh(\eta\text{-indenyl})$

			Ph[h]			indenyl			
M		T, °C	ortho	meta	para	$H_{4\text{-}7}$[c]	$H_{1,3}$[d]	H_2[e]	Cp
Zr	**1c**	95[f]	7.44	7.29	7.21	6.54, 6.05	5.63 (2.5)	6.27 (2.5)	4.93
		−60[g]	7.74, 7.09	7.72, 7.26	7.32, 7.23	6.55, 5.82	5.52 (2.5)	6.41 (2.5)	5.08, 4.83
Hf	**1d**	95[f]	7.46	7.29	7.20	6.56, 6.13	5.67 (2.5)	6.30 (2.5)	4.89
		−60[g]	7.81, 7.11	7.44, 7.27	7.32, 7.25	6.59, 5.96	5.61	6.45	5.25, 4.65

3. $[Cp_2M(\mu\text{-}PEt_2)_2Rh(CH_3)(\eta\text{-indenyl})]I$[i]

		Et		indenyl				
M	no.	CH_2	CH_3[b]	$H_{4\text{-}7}$[c]	$H_{1,3}$[d]	H_2[e]	CH_3[j]	Cp
Zr	**2a**	3.08 (mult), 2.15 (mult), 1.73 (mult), 1.37 (ov mult)	1.46 (17.0, 7.5), 1.29 (13.5, 7.0)	7.42, 7.21	6.48	5.79 (3.0)	−0.60 (3.5, 3.0)	5.61, 4.89
Hf	**2b**	3.17 (mult), 2.07 (mult), 1.74 (mult), 1.31 (ov mult)	1.45 (17.0, 7.5), 1.27 (ov mult)	7.42, 7.21	6.43	5.75 (3.0)	−0.58 (3.5, 2.5)	5.59, 4.90 (tr, $^3J_{P\text{-}H}$ = 1.5 Hz)

4. DNMR Data for Hindered Indenyl Rotation[k]

complex	T_c, K	$\Delta\nu$, Hz	k_{T_c}, s^{-1}	$\Delta G^‡_{T_c}$, kcal/mol
1a	320	181	402	15.0 ± 0.2
1b	317	182	404	14.8 ± 0.2
1c	291	77	171	14.0 ± 0.3
1d	285	59	131	13.9 ± 0.3

[a] Chemical shifts in ppm. Abbreviations: d = doublet; tr = triplet; br = broad; ov = overlapping; mult = multiplet. [b] d tr; $^3J_{P\text{-}H}$, $^3J_{H\text{-}H}$ in Hz in parentheses. [c] Multiplets due to AA′BB′ spin system. [d] d; $^3J_{H\text{-}H}$ in Hz in parentheses. [e] tr; $^2J_{Rh\text{-}H} \approx {}^3J_{H\text{-}H}$ in Hz in parentheses. [f] Run in p-dioxane-d_8. [g] Run in THF-d_8. [h] Virtual triplets with $^3J_{H\text{-}H} \approx$ 7–8 Hz. [i] Run in CD_3CN at 25 °C. [j] tr d; $^3J_{P\text{-}H}$, $^2J_{Rh\text{-}H}$ in Hz in parentheses. [k] T_c = coalescence temperature ±5 K; $\Delta\nu$ = chemical shift difference of exchanging sites ±5 Hz.

Table IV. 121-MHz ^{31}P NMR Data[a]

	no.	chem shift,[b] ppm
$Cp_2M(\mu\text{-}PR_2)_2Rh(\eta\text{-indenyl})$		
M = Zr, R = Et	**1a**	181.6 (129)
M = Hf, R = Et	**1b**	169.1 (125)
M = Zr, R = Ph	**1c**	177.3 (137)
M = Hf, R = Ph	**1d**	169.7 (133)
$[Cp_2M(\mu\text{-}PEt_2)_2Rh(CH_3)(\eta\text{-indenyl})]I$		
M = Zr	**2a**	158.5 (82)
M = Hf	**2b**	145.4 (81)

[a] Run at 25 °C with proton decoupling; **1a–d** in THF-d_8 and **2a,b** in CD_3CN. [b] All resonances are doublets; $J_{Rh\text{-}P}$ in Hz in parentheses.

product was filtered off, washed with 5 mL of hexane, and dried in vacuo, yielding 80 mg of the title complex (71%). The Hf analogue **2b** was prepared similarly by using 106 mg (0.15 mmol) of **1b**, affording 93 mg of product (74%).

X-ray Data Collection and Structure Solution and Refinement. Red crystals of complex **1c** suitable for diffraction studies were grown by slow diffusion of n-heptane into a THF solution of the complex. A crystal of appropriate dimensions (see Table VI for crystallographic details) was encapsulated in a glass capillary under N_2 and mounted on a Syntex P3 diffractometer. The crystal proved to be suitable based on Ω scans having peak widths at half-height of 0.24° at −100 °C. Preliminary photographic examination revealed the space group and approximate cell constants. The latter were refined to the values shown in Table VI by using 47 reflections chosen from diverse regions of reciprocal space.

Intensity data were collected by using the Ω scan technique (0.90° scan range, scan rates of 8–20° min^{-1}, and total background time = scan time). The intensities of three standard reflections were monitored at 200 reflection intervals and were found to vary insignificantly. The data were corrected for absorption by using the DIFABS program[7] and processed by using counting statistics and a p value of 0.02 to derive standard deviations.[8]

The solution and refinement were accomplished by using local modifications of the SDP-Plus software supplied by the Enraf-Nonius Corp. The Zr and Rh atoms were located in an origin-removed Patterson synthesis, and the positions of the remaining non-hydrogen atoms were determined by the usual combination of structure factor and Fourier syntheses and least-squares refinements. The function minimized was $\sum w(|F_o| - |F_c|)^2$, where $|F_o|$ and $|F_c|$ are the observed and calculated structure amplitudes where $w = 1/\sigma^2(F_o)$. The atomic scattering factors used were taken from the compilations of Cromer and Waber,[9a] and the anomalous dispersion terms used were Cromer's.[9b] All hydrogen atoms were located, placed in idealized positions [d(CH) = 0.95 Å], and included in the final refinements as a fixed contribution (B_H = 4.0 Å^2). Final convergence led to the agreement indices shown in Table VI where $R = \sum||F_o| - |F_c||/\sum|F_o|$ and $R_w = [\sum w(|F_o| - |F_c|)^2/\sum wF_o]^{1/2}$. The highest peak in a final difference map was adjacent to the Zr atom and corresponded to 1.58 e Å^{-3}. Other residual peaks were less than 0.35 e Å^{-3}.

Selected bond lengths and angles are compiled in Table VII. Positional and equivalent isotropic thermal parameters for the non-hydrogen atoms are collected in Table VIII. Positional and thermal parameters for the idealized hydrogen atoms (Table IX), general temperature factors (Table X), dihedral angles between calculated planes (Table XI), and structure factor amplitudes

(7) Walker, N.; Stuart, D. *Acta Crystallogr., Sect. A: Found. Crystallogr.* **1983**, *A39*, 159.
(8) Corfield, P. W.; Doedens, R. J.; Ibers, J. A. *Inorg. Chem.* **1967**, *6*, 197.
(9) "International Tables for X-ray Crystallography"; Kynoch Press: Birmingham, England, 1974; Vol IV: (a) Table 2.2B; (b) Talbe 2.3.1.

Table V. 75.6-MHz ^{13}C NMR Data[a]

1. $Cp_2M(\mu\text{-}PEt_2)_2Rh(\eta\text{-indenyl})$[b]

			indenyl[d]					ethyl[e]	
M	no.	Cp[c]	C(1,3)[f]	C(2)[g]	C(5,6)	C(4,7)	C(3a,7a)	CH_2	CH_3
Zr	1a	99.5 (172, 7)	73.9 (2.5, 169)	96.9 (7, 168)	113.8 (161)	120.7 (159)	121.3	25.0 (129)	13.6 (129)
Hf	1b	98.4 (173, 7)	73.7 (2, 172)	97.1 (4, 172)	113.8 (161)	120.5 (159)	121.1	24.9 (127)	13.6 (127)

2. $Cp_2M(\mu\text{-}PPh_2)_2Rh(\eta\text{-indenyl})$[b]

			indenyl[d]					phenyl			
M	no.	Cp	C(1,3)[f]	C(2)[g]	C(5,6)	C(4,7)	C(3a,7a)	ipso[h]	ortho[i]	meta[j]	para
Zr	1c	103.3 (br, 174)	77.4 (3.5, 173)	100.3 (6.5, 170)	117.5 (157)	123.2 (157)	127.1	145.5 (26)	134.6 (6, 160)	127.9 (5, 159)	127.5 (159)
Hf	1d	102.2 (br, 174)	76.9 (3.5, 171)	100.4 (5.5, 173)	117.6 (157)	123.0 (157)	127.5	145.6 (21)	135.0 (4, 161)	127.8 (4, 160)	127.6 (160)

3. $[Cp_2M(\mu\text{-}PEt_2)_2Rh(CH_3)(\eta\text{-indenyl})]I$[k]

			indenyl[d]						ethyl	
M	no.	Cp[c]	C(1,3)[f]	C(2)[g]	C(5,6)	C(4,7)	C(3a,7a)	CH_3[l]	CH_2[m]	CH_3
Zr	2a	104.4 (175, 7), 103.3 (175, 7)	79.6 (3.5, 179)	110.3 (6, 177)	122.6 (167)	128.2 (162)	119.8	−9.8 (26, 2.5, 139)	24.5 (17, 132)	13.9 (128)
									17.2 (14, 128)	10.8 (128)
Hf	2b	103.7 (176, 6), 102.5 (176,6)	79.3 (180)	110.0 (179)	122.6 (167)	128.0 (163)	119.5	−9.8 (26, 2.5, 139)	24.4 (8, 130)	13.9 (128)
									17.1 (9, 131)	10.9 (127)

[a] Chemical shifts in ppm. Numbering scheme:

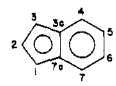

[b] Run in THF-d_8 at 60 °C with gated decoupling. [c] Doublet of virtual quintets: J_{CH}, $^2J_{CH} \approx {}^3J_{CH}$ in Hz in parentheses. [d] J_{CH} in Hz in parentheses; $^2J_{CH}$ of 5–8 Hz was also observed. [e] Broad, J_{CH} in Hz in parentheses. [f] Doublet of doublet of triplets; $J_{Rh-C} \approx {}^2J_{P-C}$, J_{CH} in Hz in parentheses. [g] Doublet of doublets; J_{Rh-C}, J_{CH} in Hz in parentheses. [h] Doublet; J_{P-C} in Hz in parentheses. [i] Doublet of doublets; $^2J_{P-C}$, J_{CH} in Hz in parentheses. [j] Doublet of doublets; $^3J_{P-C}$, J_{CH} in Hz in parentheses. [k] Run in CD_3CN at 25 °C with gated decoupling. [l] Doublet of triplet of quartets; J_{Rh-C}, $^2J_{P-C}$, J_{CH} in Hz in parentheses. [m] Doublet of triplets; J_{P-C}, J_{CH} in Hz in parentheses.

Table VI. Summary of X-ray Diffraction Data

complex	$(\eta^5\text{-}C_5H_5)_2Zr[\mu\text{-}P(C_6H_5)_2]_2\text{-}Rh(\eta\text{-}C_9H_7)$ (1c)
formula	$C_{43}H_{37}P_2RhZr$
fw	809.85
space group	C_{2h}^2—$P2_1/m$ (no. 11)
a, Å	9.700 (1)
b, Å	18.855 (3)
c, Å	10.185 (1)
β, deg	112.95 (1)
V, Å^3	1715.3 (6)
Z	2
ρ(calcd), g cm^{-3}	1.568
cryst dimens, mm	0.19 × 0.25 × 0.29
temp, °C	−100
radiatn	Mo Kα (0.71069 Å) from graphite monochromator
μ, cm^{-1}	8.94
absorptn correctn factors	0.86–1.07; av 0.99
2θ limits, deg.	4.0–55.0
total no. of unique observns	4065
data, $F_o^2 > 3\sigma(F_o^2)$	2928
final no. of variables	219
R	0.029
R_w	0.031
error in obsvn of unit wt, electrons	1.296

(Table XII) are available as supplementary material.

Results and Discussion

Synthesis of $Cp_2M(\mu\text{-}PR_2)_2Rh(\eta\text{-indenyl})$. The reaction of $Cp_2M(PR_2)_2$ with $(\eta\text{-indenyl})Rh(\eta\text{-}C_2H_4)_2$ in hexane or THF liberates ethylene, affording the new heterobimetallic complexes $Cp_2M(\mu\text{-}PR_2)_2Rh(\eta\text{-indenyl})$ (**1a–d**) in excellent yield. The products are red-orange to brown-orange, air-sensitive crystalline solids which are soluble in nonpolar organic solvents (**1c,d** are only slightly soluble in alkanes). Monitoring the reactions by ^{31}P NMR spectroscopy showed the reactions to be quantitative, although formation of **1c,d** was slow (ca. 2 days) and reaction with $Cp_2M(PCy_2)_2$ was still not clean after 1 week. Complexes **1a–d** were characterized by full elemental analysis and IR and ^1H, ^{31}P, and ^{13}C NMR spectroscopy and, for **1c**, by single-crystal X-ray diffraction.

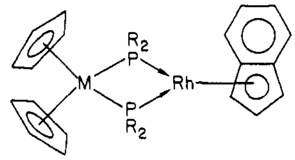

1a, M=Zr, R=Et
b, M=Hf, R=Et
c, M=Zr, R=Ph
d, M=Hf, R=Ph

Molecular Structure of $Cp_2Zr(\mu\text{-}PPh_2)_2Rh(\eta\text{-indenyl})$ (1c). The molecular structure of **1c**, shown in Figure 1, consists of edge-shared pseudotetrahedral 16e Zr(IV) and distorted square-planar Rh(I) centers with a planar ZrP_2Rh bridge system and a Zr···Rh separation of 3.088 (1) Å. A crystallographic mirror plane contains the Zr and Rh atoms and bisects the indenyl and cyclopentadienyl ligands. The indenyl ligand exhibits a pronounced "slip-fold" distortion[10] relative to a planar, η^5-indenyl ligand,[11,12] such that the Rh–C distances to the

(10) Mingos, D. M. P. In "Comprehensive Organometallic Chemistry"; Wilkinson, G., Stone, F. G. A., Abel, E. W., Eds.; Pergamon Press: Oxford, 1982; Vol. 3, Chapter 19.

(11) (a) Trotter, J. *Acta Crystallogr.* **1958**, *11*, 35. (b) Webb, N. E.; Marsh, R. A. *Ibid.* **1967**, *22*, 382. (c) Allen, S. R.; Baker, P. K.; Barnes, S. G.; Green, M.; Trollope, L.; Manojlovic-Muir, L.; Muir, K. W. *J. Chem. Soc., Dalton Trans.* **1981**, 873. (d) Allen, S. R.; Baker, P. K.; Barnes, S. G.; Bottril, M.; Green, M.; Orpen, A. G.; Williams, I. D.; Welch, A. J. *Ibid.* **1983**, 927.

Table VII. Selected Distances (Å) and Angles (deg) in $Cp_2Zr(\mu\text{-}PPh_2)_2Rh(\eta\text{-}C_9H_7)$ (1c)[a]

	Bond Distances		
Rh–Zr	3.088 (1)		
Rh–P	2.264 (1)	Zr–P	2.590 (1)
Rh–C(21)	2.249 (4)	Zr–C(31–33)	2.512–2.540 (4)
Rh–C(22)	2.242 (3)	Zr–C(41–43)	2.495–2.550 (4)
Rh–C(23)	2.469 (3)		
P–C(1)	1.838 (3)	P–C(11)	1.842 (3)
C(1–5)–C(2–6)	1.382–1.406 (5)		
C(11–15)–C(12–16)	1.377–1.402 (5)		
C(21)–C(22)	1.415 (4)	C(23)–C(24)	1.395 (4)
C(22)–C(23)	1.456 (4)	C(24)–C(25)	1.382 (4)
C(23)–C(23)′	1.443 (4)	C(25)–C(25)′	1.408 (4)
C(31–33)–C(32–33)	1.410–1.414 (4)		
C(41–43)–C(42–43)	1.400–1.408 (4)		
	Bond Angles		
Zr–Rh–P	55.33 (2)	P–Rh–P′	110.66 (3)
Zr–Rh–C(21)	151.6 (1)	P–Rh–C(21)	120.04 (4)
Zr–Rh–C(22)	148.63 (8)	P–Rh–C(22)	93.81 (8)
C(21)–Rh–C(22)	36.72 (9)	P–Rh–C(22)′	154.82 (8)
		C(22)–Rh–C(22)′	61.3 (2)
Rh–Zr–P	45.98 (2)	P–Zr–P′	91.95 (3)
Rh–Zr–C(31–33)	89.9–138.9 (1)	P–Zr–C(31–33)	82.6–136.5 (1)
Rh–Zr–C(41–43)	85.6–134.0 (1)	P–Zr–C(41–43)	80.5–133.6 (1)
Rh–P–Zr	78.70 (2)	Zr–P–C(1)	118.67 (9)
Rh–P–C(1)	114.99 (9)	Zr–P–C(11)	129.40 (9)
Rh–P–C(11)	111.48 (9)	C(1)–P–C(11)	101.9 (1)
P–C(1)–C(2)	120.5 (2)	P–C(11)–C(12)	119.6 (2)
P–C(1)–C(6)	121.1 (2)	P–C(11)–C(16)	123.2 (2)
C(2)–C(1)–C(6)	118.3 (3)	C(12)–C(11)–C(16)	117.0 (3)
C–C–C(Ph)	119.0–121.1 (3)		
Rh–C(21)–C(22)	71.4 (2)	Rh–C(22)–C(21)	71.9 (2)
C(22)–C(21)–C(22)′	107.8 (4)	Rh–C(22)–C(23)	80.7 (2)
C(22)–C(23)–C(23)′	106.8 (2)	C(21)–C(22)–C(23)	108.7 (3)
C(22)–C(23)–C(24)	133.2 (3)		
C–C–C-(benzenoid)	119.0–121.1 (3)		
C–C–C(Cp)	107.5–108.5 (4)		

[a] The prime indicates symmetry-related atoms.

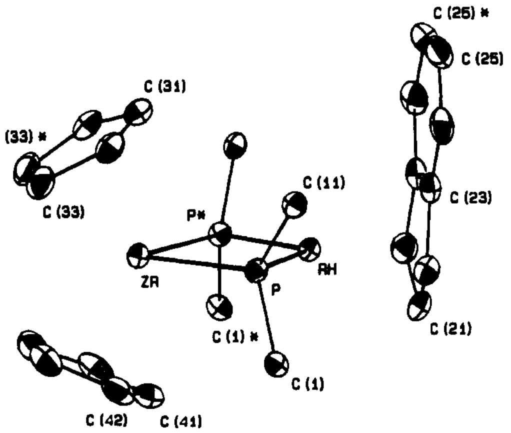

Figure 1. Molecular structure of (η-C_5H_5)$_2$Zr(μ-PPh_2)$_2$Rh(η-indenyl) (1c). Only the ipso carbon atoms of the phenyl rings are shown, and hydrogen atoms are omitted for clarity.

quaternary carbons (C(23), C(23′)) are >0.2 Å longer than those to the "allylic" carbons (C(22), C(22′)); ΔMC = 0.23 Å. The dihedral "fold" angle between the allyl and arene planes is 8.5° and the "hinge" angle about the C(22)–C(22′) vector is 10.6°, with the arene folded away from the Rh center. Although similar distortions have been observed in other rhodium– and iridium–indenyl complexes,[13] **1c** contains the most distorted indenyl ligand yet observed crystallographically,[14,34] with the exception of the η^3-indenyl ligand in (CO_2)W(η^5-indenyl)(η^3-indenyl)[12] in which ΔMC = 0.72 Å and the "fold" angle is 26°.

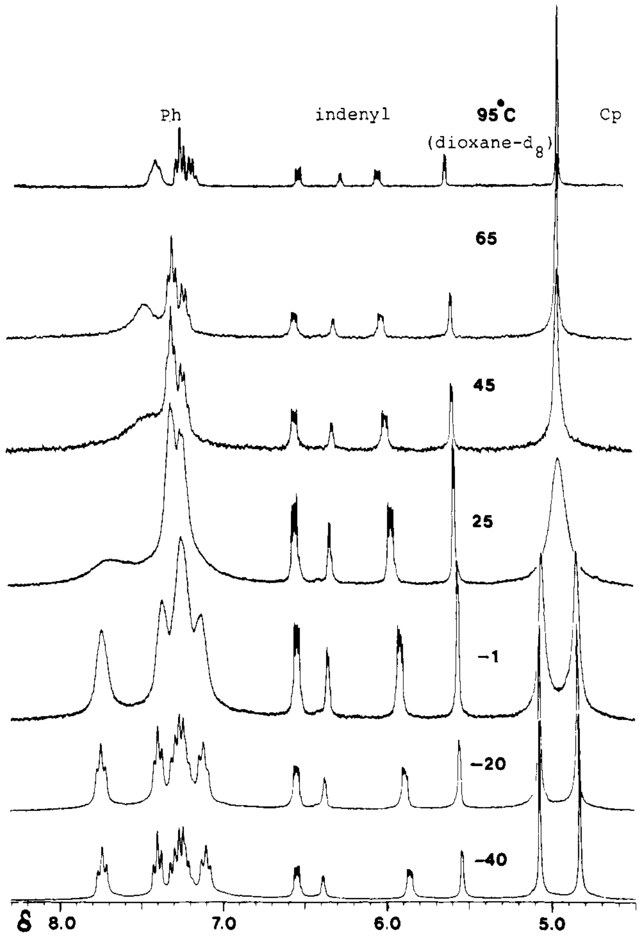

Figure 2. ^1H DNMR of (η-C_5H_5)$_2$Zr(μ-PPh_2)$_2$Rh(η-indenyl) (1c) in THF-d_8.

Spectroscopic Characterization and Hindered Indenyl Ligand Rotation. The 300-MHz ^1H NMR spectra of complexes **1a–d** at 25 °C contain sharp resonances for the indenyl ligand protons and broad resonances for the cyclopentadienyl and PR_2 protons. The series of ^1H DNMR spectra of **1c**, shown in Figure 2, show that there are two types of phenyl and cyclopentadienyl proton environments at the low-temperature limit, as expected from the observed solid-state molecular structure. At the high-temperature limit, the effective symmetry is C_{2v}, due to rapid rotation of the indenyl ligand about the Rh–Zr vector. Similarly, for **1a,b** there are two cyclopentadienyl

(12) Nesmeyanov, A. N.; Ustynyuk, N. A.; Makarova, L. G.; Andrianov, V. G.; Struchkov, Yu. T.; Andrae, S.; Ustynyuk, Yu. A.; Malyugina, S. G. *J. Organomet. Chem.* **1978**, *159*, 189.

(13) (a) Al-Obaidi, Y. N.; Green, M.; White, N. D.; Bassett, J. M.; Welch, A. J. *J. Chem. Soc., Chem. Commun.* **1981**, 494. (b) Al-Obaidi, Y. N.; Baker, P. K.; Green, M.; White, N. D.; Taylor, G. E. *J. Chem. Soc., Dalton Trans.* **1981**, 2321. (c) Al-Obaidi, Y. N.; Green, M.; White, N. D.; Taylor, G. E. *Ibid.* **1982**, *319*. (d) Green, M.; Jeffery, J. C.; Porter, S. J.; Razay, H.; Stone, F. G. A. *Ibid.* **1982**, 2475. (e) Green, M.; Howard, J. A. K.; Porter, S. J.; Stone, F. G. A.; Tyler, D. C. *Ibid.* **1984**, 2553. (f) Faller, J. W.; Crabtree, R. H.; Habib, A. *Organometallics* **1985**, *4*, 929.

(14) For [Rh(CO)(η-indenyl)]$_2$(μ-C=CH_2), ΔMC = 0.19 Å; the fold and hinge angles average 9.0 and 8.0°, respectively.[13c] For [IrH(PPh_3)$_2$(η-indenyl)]BF_4, ΔMC = 0.19 Å; the fold and hinge angles are 7.6 and 6.0°, respectively.[13f]

Table VIII. Positional Parameters and Their Estimated Standard Deviations

atom	x	y	z	B, Å²	atom	x	y	z	B, Å²
Rh	0.31972 (3)	0.250	0.64577 (3)	1.292 (6)	C(15)	0.2329 (4)	−0.0227 (2)	0.8107 (4)	2.98 (8)
Zr	0.000	0.250	0.41166 (4)	1.386 (8)	C(16)	0.2340 (3)	0.0206 (2)	0.7014 (3)	2.27 (7)
P	0.18637 (7)	0.15123 (4)	0.54808 (8)	1.39 (1)	C(21)	0.5701 (4)	0.250	0.7157 (5)	2.2 (1)
C(1)	0.2675 (3)	0.0949 (2)	0.4492 (3)	1.49 (6)	C(22)	0.5280 (3)	0.1894 (2)	0.7731 (3)	2.05 (7)
C(2)	0.3994 (3)	0.1149 (2)	0.4349 (3)	1.76 (6)	C(23)	0.4843 (3)	0.2117 (2)	0.8883 (3)	1.79 (6)
C(3)	0.4569 (3)	0.0742 (2)	0.3539 (3)	1.98 (6)	C(24)	0.4416 (3)	0.1748 (2)	0.9850 (3)	2.29 (7)
C(4)	0.3849 (3)	0.0130 (2)	0.2866 (3)	2.09 (7)	C(25)	0.4000 (4)	0.2127 (2)	1.0799 (3)	2.71 (8)
C(5)	0.2525 (3)	−0.0074 (2)	0.2998 (3)	2.09 (7)	C(31)	−0.1077 (4)	0.250	0.6025 (5)	2.10 (9)
C(6)	0.1943 (3)	0.0331 (2)	0.3793 (3)	1.84 (6)	C(32)	−0.1657 (3)	0.1891 (2)	0.5177 (3)	2.07 (6)
C(11)	0.1792 (3)	0.0899 (2)	0.6861 (3)	1.56 (6)	C(33)	−0.2595 (3)	0.2126 (2)	0.3803 (4)	2.38 (7)
C(12)	0.1258 (3)	0.1140 (2)	0.7878 (3)	2.13 (7)	C(41)	0.1258 (5)	0.250	0.2396 (5)	2.9 (1)
C(13)	0.1234 (3)	0.0697 (2)	0.8962 (3)	2.63 (7)	C(42)	0.0329 (4)	0.1898 (2)	0.2049 (3)	2.63 (7)
C(14)	0.1762 (4)	0.0012 (2)	0.9076 (4)	2.79 (8)	C(43)	−0.1162 (4)	0.2127 (2)	0.1505 (3)	2.45 (7)

[a] Anisotropically refined atoms are given in the form of the isotropic equivalent thermal parameter defined as $(^4/_3)[a^2B(1,1) + b^2B(2,2) + c^2B(3,3) + ab(\cos\gamma)B(1,2) + ac(\cos\beta)B(1,3) + bc(\cos\alpha)B(2,3)]$.

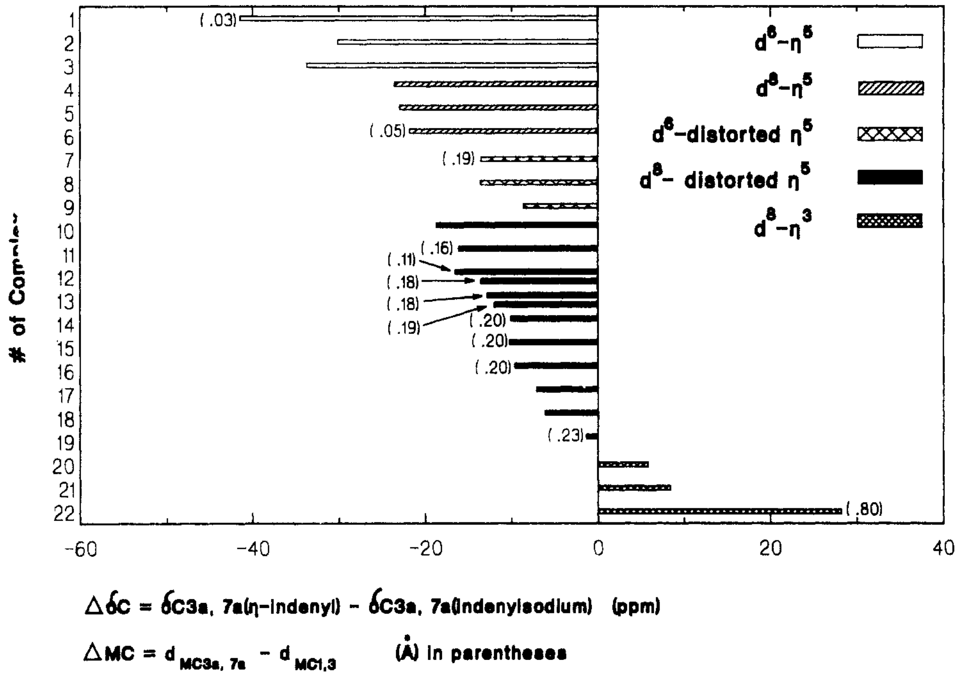

Figure 3. Correlation of ^{13}C NMR chemical shift difference, $\Delta\delta(C)$, with indenyl ligand hapticity: complex 1, $Fe(ind)_2$;[17] 2, $[Co(ind)_2]^+$;[17] 3, $[Rh(\eta\text{-}C_5Me_5)(ind)]^+$;[29] 4, $Co[P(OEt)_3]_2(ind)$;[1i] 5, Co(1,5-COD)(ind);[30] 6, Rh(duroquinone)(ind);[31,32] 7, $[IrH(PPh_3)_2(ind)]^+$;[13f] 8, $[Rh(Me)(PMe_3)_2(ind)]^+$;[32] 9, $[Cp_2Zr(\mu\text{-}PEt_2)_2Rh(Me)(ind)]^+$ (**2a**); 10, Ir(1,5-COD)(ind);[33,34] 11, $Rh(\mu\text{-}C_2H_4)_2(ind)$;[1d,32] 12, $[Rh(ind)]_2(\mu\text{-}CO)(\mu\text{-}1,3\text{-}CHD)$;[13a] 13, $[Rh(CO)(ind)]_2(\mu\text{-}C{=}CH_2)$;[13c] 14, $Rh(CO)_2(ind)$;[1k] 15, $Rh(CN\text{-}t\text{-}Bu_2)_2(ind)$;[32] 16, $Rh(PMe_3)_2(ind)$;[32] 17, $Cp_2Zr(\mu\text{-}PEt_2)_2Rh(ind)$ (**1a**); 18, $Cp_2Zr(\mu\text{-}PEt_2)_2Ir(ind)$;[35] 19, $Cp_2Zr(\mu\text{-}PPh_2)_2Rh(ind)$ (**1c**); 20, $Ni(ind)_2$;[17] 21, $[PdCl(ind)]_2$;[36] 22, $Ir(PMe_2Ph)_3(ind)$[34] (COD = cyclooctadiene and CHD = cyclohexadiene). ΔMC value for complex 1 is for $Ru(ind)_2$[11b] as X-ray data for $Fe(ind)_2$[11a] are of insufficient accuracy.

and four methylene proton environments at low temperature, which average to one and two unique environments, respectively, at 90 °C. Application of the Eyring equation[15] for two-site exchange of the cyclopentadienyl protons gives the following values of the free energy of activation: $\Delta G^{\ddagger}_{T_c} = 15.0 \pm 0.2, 14.8 \pm 0.2, 14.0 \pm 0.3$, and 13.9 ± 0.3 kcal/mol, respectively, for **1a–d**. The only other report[16] of hindered indenyl rotation is for the thermally unstable heterobimetallic complex $(\eta\text{-mesityl})Cr(CO)(\mu\text{-}CO)_2Rh(CO)(\eta\text{-indenyl})$, for which $\Delta G^{\ddagger}_{T_c} = 10.8 \pm 0.2$ kcal/mol. It was suggested that the magnitude of the observed barrier is a result of the "slip-fold" distortion of the η-indenyl ligand.

The ^{13}C NMR spectra of **1a–d** are consistent with the above analysis and suggest that the "slip-fold" distortion of the coordinated indenyl ligand persists in solution. Kohler[17] has noted that the hapticity of the indenyl ligand can be assessed spectroscopically by comparing the NMR chemical shifts of the five-membered ring carbon atoms in the metal complex with those of indene; for η^3-indenyl ligands C(1–3) are shielded while C(3a,7a) are not. For more quantitative comparisons, we have calculated the chemical shift difference, $\Delta\delta(C) = \delta(C(\eta\text{-indenyl})) - \delta(C(\text{indenyl sodium}))$, for those d^6 and d^8 complexes for which ^{13}C NMR data are available (Figure 3). The $\Delta\delta(C)$ values for C(3a,7a) correlate well with the hapticity of the indenyl ligand for those examples for which structural and/or theoretical results are also available. $\Delta\delta(C(3a,7a)) = -20$ to -40 ppm for planar η^5-indenyl, -10 to -20 ppm for distorted η^5-indenyl, and $+5$ to $+30$ ppm for η^3-indenyl ligands. The values for **1a–d** range from 0 to −10 ppm, again pointing to a severely distorted η^5-indenyl ligand. While we may speculate that the severity of the "slip-fold" distortion is responsible for the large observed barriers to indenyl ligand rotation, more structural and theoretical

(15) Martin, M. L.; Martin, G. J.; Delpeuch, J.-J. "Practical NMR Spectroscopy"; Heyden: Philadelphia, 1980; Chapter 8, p 339.
(16) Barr, R. D.; Green, M.; Marder, T. B.; Stone, F. G. A. *J. Chem. Soc., Dalton Trans.* **1984**, 1261.
(17) Kohler, F. H. *Chem. Ber.* **1974**, *107*, 570.

work[18] on analogous systems is required for an understanding of the electronic contributions to the rotational barrier.

The ^{31}P NMR spectra of complexes **1a–d** consist of a doublet at 170–180 ppm (J_{Rh-P} = 125–137 Hz), in good accord with other $Cp_2M(\mu\text{-}PR_2)_2M'L_n$ complexes.[4,6,19,20] The low value of J_{Rh-P} is typical for Rh(μ-PR_2)M′ bridges.[21-23]

The IR spectra of **1a–d** contain absorptions due to cyclopentadienyl,[24,25] indenyl,[25] and PR_2 ligands.[2] The only absorptions that change significantly going from Zr to Hf complexes are observed below 400 cm^{-1} (Table II) and presumably involve M–P vibrations.[24,26]

Synthesis and Characterization of [$Cp_2M(\mu$-$PEt_2)_2Rh(CH_3)$(η-indenyl)]I. Werner and Feser[27] showed that $Rh(PMe_3)_2$(η-indenyl) undergoes oxidative addition reactions with CH_3I and $CH_3C(O)Cl$, affording the cationic Rh(III) complexes [$RhR(PMe_3)_2$(η-indenyl)]$^+$ (R = CH_3, $C(O)CH_3$). Addition of 1 equiv of CH_3I to complexes **1a,b** in benzene led to precipitation of the yellow 1:1 adducts in quantitative yield. Elemental analysis and infrared and NMR spectroscopic characterization showed the adducts to be iodide salts of the d^0–d^6 heterobimetallic cations [$Cp_2M(\mu$-$PEt_2)_2Rh(CH_3)$(indenyl)]I (**2a,b**). The Rh–CH_3 moiety was characterized by a doublet of triplets at δ –0.6 ($J_{HRh} \approx {}^3J_{HP}$ = 3 Hz) in the ^{1}H NMR and a quartet of doublets of triplets at –10 ppm (J_{CH} = 139, J_{CRh} = 26, and $^2J_{CP}$ = 2.5 Hz) in the ^{13}C NMR. The ^{31}P NMR spectra of **2a** (**2b**) in CD_3CN consisted of a doublet at 158.5 (145.4) ppm with J_{PRh} = 82 (81) Hz. Although **1a,b** do not react with 1 atm of H_2 or CO or with $CH_3C(O)Cl$, reactions are observed with $CH_3C(O)Br$ and with NH_4PF_6 which alter the MP_2Rh bridge system without complete disruption.[28] These studies will appear separately.

Acknowledgment. We wish to thank S. A. Hill and L. F. Lardear for excellent technical assistance, Dr. T. B. Marder for useful discussions, and Dr. J. S. Merola and Professors R. A. Crabtree and J. W. Faller for communication of results prior to publication.

Registry No. 1a, 100113-58-4; 1b, 100113-59-5; 1c, 100113-60-8; 1d, 100113-61-9; 2a, 100113-62-0; 2b, 100113-63-1; $Cp_2Zr(PEt_2)_2$, 86013-23-2; (η-indenyl)Rh(η-C_2H_4)$_2$, 63428-46-6; $Cp_2Hf(PEt_2)_2$, 86013-26-5; $Cp_2Zr(PPh_2)_2$, 86013-25-4; $Cp_2Hf(PPh_2)_2$, 86013-28-7.

Supplementary Material Available: Tables of non-hydrogen atom thermal parameters (Table IX), idealized hydrogen atom positions (Table X), plane data (Table XI), and a listing of observed and calculated structure factor amplitudes (Table XII) and the data (Table XIII) for Figure 3 (23 pages). Ordering information is given on any current masthead page.

(18) A combined theoretical (EHMO), X-ray structural, and DNMR spectroscopic (with the η-1-Me-indenyl ligand) study is presently underway: Marder, T. B.; Calabrese, J. C.; Roe, D. C.; Tulip, T. H., to be submitted for publication.

(19) Stelzer, O.; Unger, E. *Chem. Ber.* **1977**, *110*, 3430. Johannsen, G.; Stelzer, O. *Ibid.* **1977**, *110*, 3438.

(20) Targos, T. S.; Rosen, R. P.; Whittle, R. R.; Geoffroy, G. L. *Inorg. Chem.* **1985**, *24*, 1375.

(21) Kreter, P. E.; Meek, D. W. *Inorg. Chem.* **1983**, *22*, 319.

(22) Breen, M. J.; Geoffroy, G. L. *Organometallics* **1982**, *1*, 1437. Breen, M. J.; DeBrosse, C. W.; Duttera, M. R.; Geoffroy, G. L.; Morrison, E. D.; Roberts, D. A.; Shulman, P. M.; Steinmetz, G. R.; Whittle, R. R. *Ibid.* **1983**, *2*, 846. Burkhardt, E. W.; Mercer, W. C.; Geoffroy, G. L. *Inorg. Chem.* **1984**, *23*, 1779.

(23) Jones, R. A.; Wright, T. C.; Atwood, J. L.; Hunter, W. E. *Organometallics* **1983**, *2*, 470. Jones, R. A.; Wright, T. C. *Ibid.* **1983**, *2*, 1842. Atwood, J. L.; Hunter, W. E.; Jones, R. A.; Wright, T. C. *Inorg. Chem.* **1983**, *22*, 993. Jones, R. A.; Lasch, J. G.; Norman, N. C.; Stuart, A. L.; Wright, T. C.; Whittlesey, B. R. *Organometallics* **1984**, *3*, 114. Chandler, D. J.; Jones, R. A.; Stuart, A. L.; Wright, T. C. *Ibid.* **1984**, *3*, 1830.

(24) Nakamoto, K. N. "Infrared and Raman Spectra of Inorganic and Coordination Compounds", 3rd ed.; Wiley-Interscience: New York, 1978; pp 330–335.

(25) Samuel, E.; Bigorgne, M. *J. Organomet. Chem.* **1971**, *30*, 235.

(26) Ferraro, J. R. "Low-Frequency Vibrations of Inorganic and Coordination Compounds"; Plenum Press: New York, 1971; pp 257–261.

(27) Werner, H.; Feser, R. *Z. Naturforsch., B: Anorg. Chem., Org. Chem.* **1980**, *35B*, 689.

(28) Other examples of reactions at PR_2 bridges which do not lead to fragmentation to mononuclear species include: Carty, A. J. *Pure Appl. Chem.* **1982**, *113*, 54; *Adv. Chem. Ser.* **1982**, *No. 196*, 163. Collman, J. P.; Rothrock, R. K.; Finke, R. G.; Moore, E. J.; Rose-Munch, F. *Inorg. Chem.* **1982**, *21*, 146. Klingert, B.; Werner, H. *J. Organomet. Chem.* **1983**, *252*, C47. Yu, Y.-F.; Galluci, J.; Wojcicki, A. *J. Am. Chem. Soc.* **1983**, *105*, 4826. Yu, Y.-F.; Chau, C.-N.; Wojcicki, A.; Calligaris, M.; Nardin, G.; Balducci, G. *Ibid.* **1984**, *106*, 3704. Shyu, S.-G.; Wojcicki, A. *Organometallics* **1984**, *3*, 809. Henrick, K.; Iggo, J. A.; Mays, M. J.; Raithby, P. R. *J. Chem. Soc., Chem. Commun.* **1984**, 209. Rosenberg, S.; Whittle, R. R.; Geoffroy, G. L. *J. Am. Chem. Soc.* **1984**, *106*, 5934.

(29) White, C.; Thompson, S. J.; Maitlis, P. M. *J. Chem. Soc., Chem. Commun.* **1976**, 409.

(30) Bonneman, H.; Samson, M. Canada Patent 1130289 (Studiengesellschaft Kohle m.b.H.), 1982.

(31) Aleksandrov, G. G.; Struchkov, Yu. T. *Zh. Strukt. Khim.* **1971**, *12*, 120.

(32) Marder, T. B., private communication.

(33) Sievert, A. C. Ph.D. Thesis, University of California, 1980.

(34) The X-ray structure of $Ir(PMe_2Ph)_3(\eta^3$-indenyl) has recently been determined: ΔMC = 0.80 Å and the "fold" angle is 28.5°. Merola, J. S., private communication.

(35) Baker, R. T., unpublished results.

(36) Nakasuji, K.; Yamaguchi, M.; Murata, I.; Tatsumi, K. Nakamura, A. *Organometallics* **1984**, *3*, 1257.